Available online www.jocpr.com

Journal of Chemical and Pharmaceutical Research, 2019, 11(12):45-65

Research Article

ISSN: 0975-7384
CODEN(USA): JCPRC5

Thermal and Radiochemical Analysis of Some Nucleic Acid Complexes

Mamdouh S Masoud[1], Ahmed S El-Kholany[2*] and Mohamed F El-Shahat[3]

[1]*Chemistry Department, Faculty of Science, Alexandria University, Alexandria, Egypt*

[2]*Medical Laboratory Department, Faculty of Allied Medical Sciences, Pharos University in Alexandria, Egypt*

[3]*Chemistry Department, Faculty of Science, Ain Shams University, Cairo, Egypt*

ABSTRACT

The complexes of thiobarbituric acid and adenine with Mn (II), Mo(VI) and Cr(III) were prepared. The structures, mode of bonding and the geometry of the prepared complexes were characterized by the elemental analysis, IR and electronic spectroscopy. Thermal studies were carried for the prepared complexes. The mechanisms of the thermal decomposition for the prepared complexes were studied by TGA. Thermodynamic and kinetic studies of the complexes were determined by DTA, and DSC techniques. The influences of the structural properties of the chelating agent and the type of the metal on the thermal behavior of the complexes, the order (n) , the heat of activation (E) , The collisions number (Z) and The change of entropy values (ΔS#) of the various decomposition stages were determined from the TG and DTA. The reaction of some of the prepared complexes with 18F-in different media was studied. Characterization of the 18F-complexes and the determination of the extent of radiolabeling was done by thin layer chromatography using (95:5) acetonitrile to water solution as a solvent.

Keywords: Adenine; Thiobarbituric acid; Chelating agent

INTRODUCTION

Pyrimidine derivatives constitute an important class of compounds because they are components of the biologically nucleic acid. They have been shown to exert pronounced physiological effects [1]. Barbituric acid derivatives are well-known class of compounds where many of which are widely used as drugs having pharmacological activities as depressants, hypnotics and stimulants [2]. In our laboratory extensive studies were recorded for the coordination chemistry of some nucleic acid compounds [3-5].

Molybdenum is a second-row transition metal ion that is involved in any sort of biological activity. In particular, through its +4, +5 and +6 oxidation states, it plays an important role in various oxido reductase enzymes [6-8].

The coordination chemistry of manganese (II) has attracted considerable interest due to the crucial role played by the metal in redox and non-redox proteins. Studies involving the synthesis and characterization of manganese

complexes are useful towards the understanding of the structure and reactivity of manganese sites in biological systems [9-11].

A large number of chromium (III) compounds are known. Chromium (III) complexes of macrocyclic ligands are well known for their biological importance as well as their anticarcinogenic, antibacterial and anti-fungal properties [12]. There are numerous Cr (III) complexes, which have been well characterized, providing a fertile set of model small molecule oxidants for inquiry. Cr (III) complexes with O, N and S donor macrocyclic ligands can increase the activity of insulin by binding to a small chromium binding protein [13]. Chromium (III) ions tend to form octahedral complexes. The colors of these complexes are determined by the ligands attached to the Cr center [14].

Molecules labelled with the unnatural isotope fluorine-18 are used for positron emission tomography. Molecular imaging technology is not exploited at its full potential because many 18F-labelled probes are inaccessible or notoriously difficult to produce. Typical challenges associated with 18F radiochemistry are the short half-life of 18F (<2 h), the use of sub-stoichiometric amounts of 18F, relative to the precursor and other reagents, as well as the limited availability of parent 18F sources of suitable reactivity ([18F] F-and [18F] F2) [15].

The positron-emitting radiopharmaceuticals are of particular interest due to the high sensitivity and excellent resolution of the Positron Emission Tomography (PET). These radiopharmaceuticals are formulated from cyclotron-produced or generator-eluted radionuclides should be subjected to Quality Control (QC) tests to assure their safety and efficacy before injecting to the patient. Fluorine-18 fluorodeoxyglucose (F-18 FDG), a glucose analog, is the most popular PET radiopharmaceutical. Apart from F-18 FDG, few other radionuclides such as C-11, N-13, O-15, Ga-68, I-124, and Cu-64, and so on are also being used for PET imaging [16].

Aim of the Work

1) Synthesis of Thiobarbituric acid and adenine with Mn(II), Mo(VI) and Cr(III) complexes.
2) Determination of the structure for the prepared complexes (geometry and mode of bonding) based on elemental analyses and spectral results.
3) Thermal studies of some of the prepared complexes using DTA, TGA and DSC techniques.
4) Studying the reaction of 18F-with some of the prepared complexes at different media.

EXPERIMENTAL SECTION

1) Synthesis of the Complexes

a) Preparation of Cr(III) and Mo(VI) adenine complexes: A hot clear solution of 0.01 mole of chromiom (III) sulfate salt in 25 ml water was added to 0.01 mole solution of adenine dissolved in 25 ml of hot ethanol for preparation of Cr_2 $(HL^1)_2(H_2L^1)$ $(SO_4)_2$ $(H_2O)_7$ and hot clear solution of 0.01 mole of ammonium molybdate salt in 25 ml water was added to 0.01 mole solution of adenine dissolved in 25 ml of hot ethanol for preparation of Mo_2 $(L^1)_5(OH)_2$ $(H_2O)_3$ complex. The reaction was done in presence of 5 ml concentrated ammonia solution. The reaction mixture was refluxed for 45 min and the precipitated complexes were filtered, washed several times by water and dried in a desiccator over $CaCl_2$. The elemental analyses are given in (Table 1).

Table 1. Elemental analyses of adenine (H_2L^1) complexes, found () and calculated

Complex	%M	%H	%N	%C	%S
Cr_2 $(HL_1)_2(H_2L_1)$ (SO_4) $_2(H_2O)_7$	Cr				
	-12.29	-3.69	(11.83)12.05	-22.55	-7.56
	12.39	3.48		22.89	7.67
Mo_2 $(L_1)_5(OH)_2$ $(H_2O)_3$	Mo				
	-19.86	-36.08	(36.08)36.46	-2.56	
	19.89	36.46		2.73	

b) Preparation of Cr(III), Mn(II) and Mo(VI) thiobarbituric acid complexes: A 0.01 mole solution of thio barbituric acid dissolved in ethanol was added to a hot clear solution of 0.01 mole chromium (III) sulfate salt in 25 ml water, hot clear solution of 0.01 mole $MnCl_2.4H_2O$ salt in 25 ml water and hot clear solution of 0.01 mole of ammonium molybdate salt in 25 ml water for preparation of Cr (HL^2) (L^2) $(H_2O)_3$, Mn $(H_2L^2)_3Cl_2$ and $Mo_2(L^2)5(HL^2)_2$ complexes respectively. The reactions were done in presence of 5 ml concentrated ammonia solution. The reaction mixtures were refluxed for 45 min and the precipitated complexes were filtered, washed several times by water and dried in a desiccator over $CaCl_2$. The elemental analyses are given in Table 2.

Table 2. Elemental analyses of thiobarbituric acid (H_2L^2) complexes, calculated and found ()

Complex	%M	%H	%N	%C	%S	%Cl
Cr $(H\ L^2)(L^2)$ $(H_2O)_3$	Cr			(24.28) 24.62		
	-13.16	-2.62	-13.93		-16.4	
	13.32	2.58	14.35		16.43	
Mn $(H_2\ L^2)_3Cl_2$	Mn			(25.61)25.82		
	-9.34	-2.14	-14.33		-17.07	-12.24
	9.84	2.17	15.05		17.32	12.7
$Mo_2(L^2)_5(H\ L^2)_2$	Mo			(28.59)27.96		
	-16.54	-2.49	-18		-20.23	
	15.95	2.51	18.13		20.77	

2) Chemical Analyses

a) Carbon, hydrogen, nitrogen, sulphur and halogen analyses: The measurements have been carried out at the micro-analytical laboratory at the Chemistry Department Faculty of Science, Cairo University.

b) Metal analyses: Mn and Cr complexes were digested in aquaregia and the digested products were determined by the atomic absorption technique at the Central Laboratory, Faculty of Science, Alexandria University.

Mo complexes were digested in aqua regia then ICP/MS technique at The Main Laboratory of the Chemical War, Ministry of Defense, Cairo, Egypt, was used for Mo determination.

3) Spectrophotometeric Measurements

Nujol mull ultraviolet and visible spectra: the solid complexes were measured by Perkin Elmer Lambda 4.B UVLVIS, Spectrophotometer at the Central Laboratory, Faculty of Science, Alexandria University.

4) Infrared Spectra

The data have been carried out by Bruker Tensor 37 FTIR spectrometer, KBr dick technique at the Central Laboratory, Faculty of Science, Alexandria University.

5) Thermal Analyses Measurements

The measurements have been carried out by SDT Q600. Simultaneous TGAL DSC, USA, at nitrogen atmosphere, rate of heating 10 C°/min at the micro-analytical laboratory at the Chemistry Department Faculty of Science, Cairo University.

6) The Reaction of ^{18}F with Some of the Prepared Complexes

a) **Preparation of $^{18}F^-$:** It was synthesized by proton bombardment of Oxygen-18 enriched water from CTI 18 Mev cyclotron after 30 min of proton bombardment to18O-enriched water. The synthesized 18F was transferred to the chemistry module (CPCU) (Chemistry module produced by CTI) through shielded capillary tubes.

$^{18}F^-$ was collected by light QMA (Quaternary ammonium anion exchange) Sep-Pak column (Accell Plus QMA Sep-PakTM). The retained 18F is then eluted with an acetonitrile solution of Kryptofix and potassium carbonate.

b) The interaction of ^{18}F with some of the prepared complexes: About 50 mCi from the freshly prepared ^{18}F solution was added to 2 ml (0.01 mole) of the Mn $(H_2L^2)_3Cl_2$, Mo_2 $(L^3)_5(OH)_2$ $(H_2O)_3$, MoO_2 $(HL)_2$, Cr (H L^2)(L_2) $(H_2O)_3$, Cr $(HL^4)_2$ ($(H_2O)(OH)$ and Cr_2 $(HL^3)_2(H_2L^3)$ $(SO_4)_2(H_2O)_7$ complexes, each reaction mixture was divided into three vessels, 1 ml of HCl (30%) was added to the first vessel, while 1 ml of (30%) ammonia solution was added to the second vessel, while the third vessel remain without any additions.

The silica gel plates (Whatman 250 µm layer) were used for thin layer chromatography, 5µl of reaction mixture solutions was spotted on (0.8 x 10 cm) TLC plate, which was then placed into chamber and developed by solution (95: 5 water to acetonitrile) to the top of the plate, finally the plate was dried. Radio detector (Bioscan-AR-2000) was used to identify the position of the radioactive spots, to determine both the percentage of the activity (automatically by calculating the areas under the peaks) and the R_f values of the spots on the plate.

RESULTS AND DISCUSSION

IR Spectra of Adenine Complexes

The reaction of adenine with Mo (VI) and Cr (III), Table 3 and Figure 1 is verified by the disappearance of stretching bands at (3360-3296 cm^{-1}) and bending band at 1673 cm^{-1} of NH which indicates the contribution of NH in complexation. For the NH_2 group, two absorption bands within 3300-3500 cm^{-1} in the free ligand, was assigned at low-frequency upon coordination and appeared as one broad band at 3434, 3416 for Mo and Cr complexes respectively may be due to the overlap of the NH_2, coordinated H_2O bonds [17].

The shift of the absorption bands associated with the stretching and bending vibrations of C=C and C=N groups in the purine ring, in the complexes, the C=C and C=N stretching vibrations are observed at 1480 cm (in adenine, at 1508 cm^{-1}) and the bending vibrations at 1123 and 796-760 cm (in adenine, at 1024 and 847-873 cm^{-1}), signifying that the metal ion has interacted with one heterocyclic nitrogen atom [18].

The imidazole ring frequencies (1419, 1334 and 1309 cm^{-1}) and pyrimidine ring frequencies (1605 and 1451 cm^{-1}) in the spectrum of free adenine are shifted to lower wave numbers, with reduction of intensity in the spectra of complexes indicating deprotonating and bridging of the adenine [19].

The appearance of a sharp band at 1133 cm^{-1} and a weak band at 994 cm^{-1} represent of SO_4 for Cr complex provides that SO_4 group acts as a bidentate ligand [20].

The appearance of weak bands at 512 cm^{-1} for Mo complex and 525 cm^{-1} for Cr complex provides a strong evidence for the formation of M-N bond.

Table 3. IR spectra in cm^{-1} of adenine (H_2L^1), Mo_2 $(L^1)_5(OH)_2$ $(H_2O)_3$ and Cr_2 $(H\ L^1)_2(H_2\ L^1)$ $(SO_4)_2(H_2O)_5$

Adenine	Mo_2 $(L^1)_5(OH)_2$ $(H_2O)_3$	Cr_2 $(H\ L^1)_2(H_2\ L^1)$ $(SO_4)_2(H_2O)_7$	Assignment
3467-3360	3434	3416	ν NH_2
3269-3119	-	-	ν NH
2980	2923	2900	ν N=CH
1673			δ NH_2
1605-1508-1451	1588-1480	1618-1480	ν C=C, ν C=N
1419-1369-1334	1425-1337	1415-1373	ν C=C, ν C=N
		-1333	ν_3 SO_4
1024-940-912	1023-941-910	994	δ C=C, δ C=N, ν_1 SO_4
874-797	796-760	796-760	δ C=C, δ C=N
-	512	525	ν M-N

Thiobarbituric Acid Complexes

The IR spectrum of thiobarbituric acid in the solid state does not contain ν SH band, indicating that the ligand does not contain free SH group in the solid state. The presence of very weak band at 2580 cm^{-1} indicates that the proportion of hydrogen bonded thiol is much less in the solid state than the concentration of the thione [21] A comparison of the IR spectra of the ligand and the metal complexes, Table 4 brings out the following facts:

1-The spectra of the solid complexes exhibited a broad band at 3500-3400 cm^{-1}, which attributed to ν OH of the associated water molecules, while the band observed at 860-740 cm^{-1} is assigned to coordinated water molecules [22].

2-The carbonyl absorption band ν C=O of the ligand at 1691 cm^{-1} disappeared as in Mo^{+6} and Cr^{+3} complexes or shifted to lower frequency and becomes of weak appearance in the spectrum of Mn^{+2} complex. The change in the carbonyl band both in position and intensity indicated that at least one of the two carbonyl groups in the

thiobarbituric acid compound is coordinated to these metal ions. However, the ν NH band at 3238 cm^{-1} was almost disappeared in the spectra of Mo^{+6}, Mn^{+2} and Cr^{+3} complexes suggesting that the NH groups are either (i) participate in bond formation with the metal ions; or (ii) tautomerized with the adjacent groups to form the enol-thiol tautomer.

3-The appearance of ν OH, ν C=N, ν C-O and ν C-S in the frequency at 2921, 1641, 1398 and 800 cm^{-1}, respectively, is strong evidence that the ligand is tautomerized to the enol thiol structure before complexation with the metal ions [23]. The appearance of weak bands at 537 and 533 cm^{-1} for Mo^{+6}, Mn^{+2} and Cr+3 complexes respectively provides a strong evidence for the formation of M-N bond [24].

Table 4. IR spectra in cm^{-1} of thiobarbituric acid (H_2L^2), $Mo_2(L^2)_5$ $(H\ L^2)_2$, Mn $(H_2L^2)_3Cl_2$ and Cr $(H\ L^2)$ (L^2) $(H_2O)_3$

Thiobarbituric acid	$Mo_2(L^2)_5(H\ L^2)_2$	Mn $(H_2\ L^2)_3Cl_2$	Cr $(H\ L^2)(L^2)$ $(H_2O)_3$	Assignment
3459	3419	3421	3468	ν OH
3238	-	-	-	ν NH
2921	29242859	2918	-	ν OH, ν SH
2580	-	-	-	ν C=S
1691	-	1703	-	ν C=O
1641	1639	1627	1643	ν C=N
1461	1425	1428	1454	δ NH
1398	1362	1374	1401	ν (C–O),
1151	1120	1154	-	ν C=S+ν C=N
1351	1282	1339	1303	δ O-H
1156	1120	1154		ν (CS)+ν (CN)
				CCH
800	798	780	792	ν X–Σ
-	525	537	533	ν M-N

Nujol Mull Spectra

The electronic spectrum for the prepared complexes was given in Table 5.

1-Molybdenum complexes: The $Mo_2(\mathbf{L^2})_5(H\ \mathbf{L^2})_2$ and Mo_2 $(\mathbf{L^2})_5(OH)_2$ $(H_2O)_5$ complexes gave bands at (235, 264, 335 and 410 nm) and (325, 358, 394) respectively. The absorption bands between 200 and 400 nm can be assigned to ligand to metal charge transfer (CT) transitions [25], while the absorption band at 330 nm for 335 nm for $Mo_2(\mathbf{L^2})_5(H\ \mathbf{L^2})_2$ and 325 for Mo_2 $(L^1)_5(OH)_2$ $(H_2O)_5$ has been assigned to an octahedral geometry of molybdenum centers [26,27].

2-Manganese complexes: The Mn $(H_2\ \mathbf{L^2})_3Cl_2$ complex shows bands at (352 nm) can be assigned to metal charge transfer (CT) [28-30]. While the absorption bands at 393 nm and 575 nm corresponding to $^6A_{1g} \rightarrow {}^4E_g$, $^4A_{1g}$ and $^6A_{1g} \rightarrow {}^4T_{1g}$ (P) ν_3 transitions respectively that assigned to an octahedral manganese (II) complex [31,32].

3-Chromium complexes: The electronic spectra of Cr $(H\ L^2)(L^2)$ $(H_2O)_3$ and Cr_2 $(HL^1)_2(H_2L^1)$ $(SO_4)_2(H_2O)_7$ could be explained as follow: broad bands at were observed at 612 and 600 nm for Cr $(H\ \mathbf{L^2})_2(H_2O)_2$ and Cr_2 $(H\ L^1)_2(H_2\ L^1)$ $(SO_4)_2(H_2O)_7$ complexes respectively that could be assigned to $^4A_{2g} \rightarrow {}^4T_{2g}$, ν_1 while the absorption bands at (402, 450 nm) and (9310, 280 nm) for of Cr $(H\ L^2)(L^2)$ $(H_2O)_2$ and Cr_2 $(H\ \mathbf{L^1})_2(\mathbf{H_2\ L^1})$ $(\mathbf{SO_4})_2(\mathbf{H_2O})_7$ complexes

respectively were assigned to ($^4A_{2g} \rightarrow {}^4T_{1g}$ (ν_2 and ν_3) transitions that confirm the octahedral geometry of the complexes [33,34].

Table 5. λ max (nm) of the complexes of thiobarbituric acid (H_2L^2) and adenine (H_2L^1)

Complex	λ max (nm)
$Mo_2(L^2)_5(H\,L^2)_2$	235(s), 264(b), 335(b), 410(b)
$Mn_3(L^1)_2\,(OH)\,(H_2O)_6Cl$	375(s),539(b), 653(b)
$Mn\,(H_2\,L^2)_3Cl_2$	237(b), 352(s), 393(b),575(b)
$Cr\,(H\,L^2)(\,L^2)\,(H_2O)_3$	242, 310, 402, 612
$Cr_2\,(H\,L^1)_2(H_2\,L^1)\,(SO_4)_2(H_2O)_7$	280, 319, 364,450, 600

4-Thermal analysis: Thermal studies (DTA, TGA and DSC) were carried out for some of the prepared complexes, some representative examples for Mo and Cr complexes are given, Figures 1 and 2.

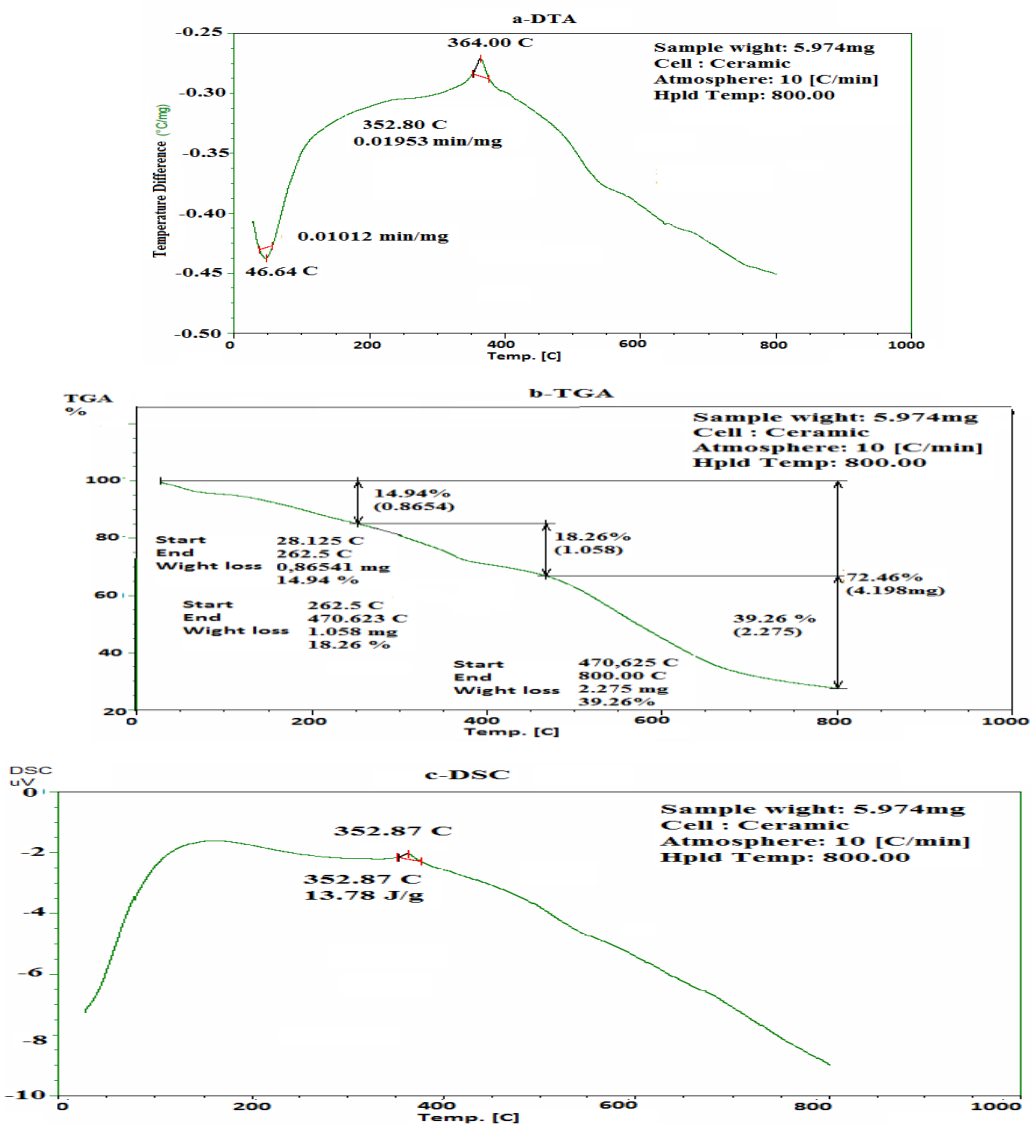

Figure 1. Thermal analysis data DTA, TGA, and DSC of $Mo_2\,(L^1)_5(OH)_2\,(H_2O)_3$

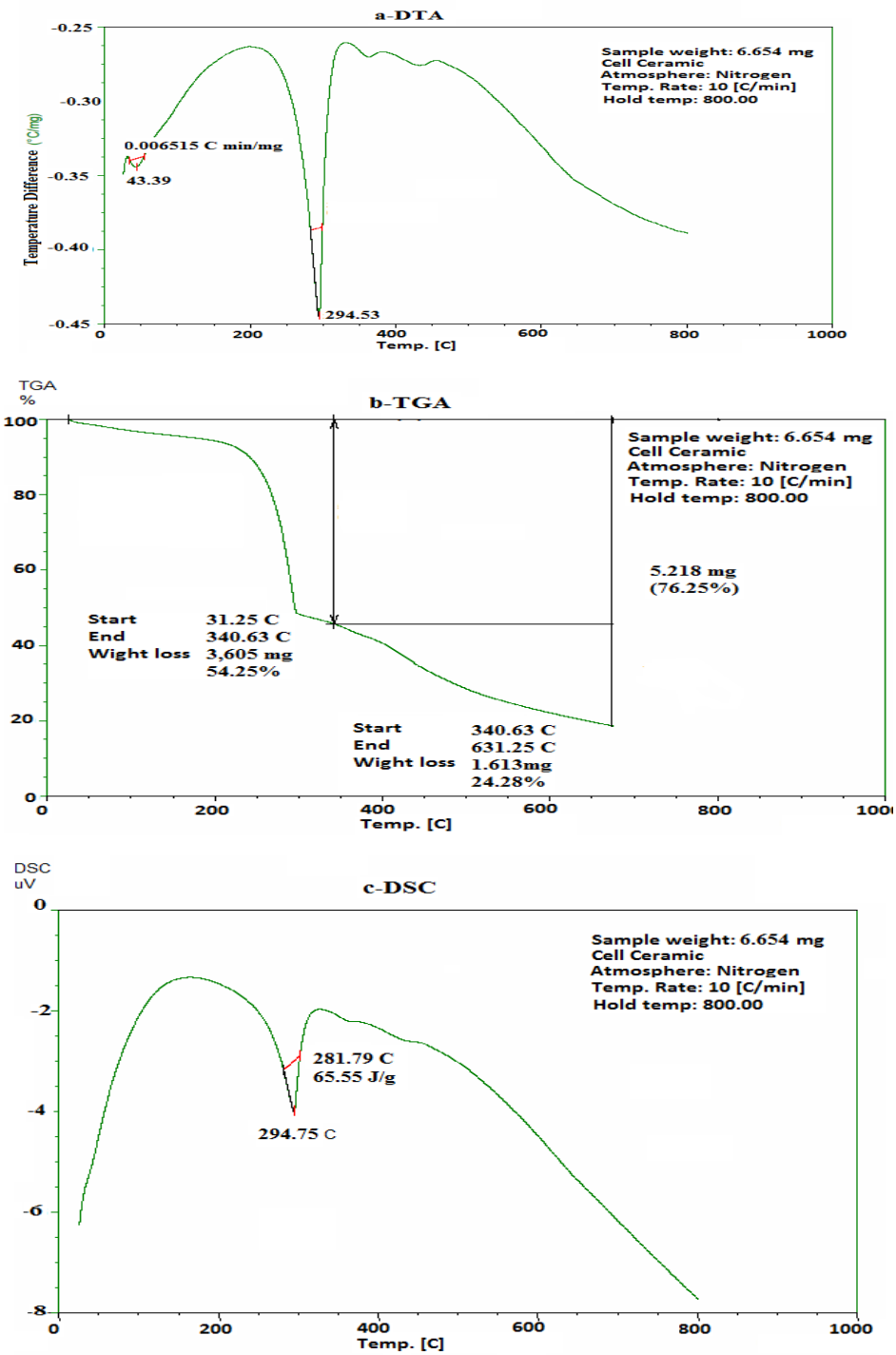

Figure 2. Thermal analysis data DTA, TGA and DSC of Cr (H L^2) (L^2) $(H_2O)_3$

a) Mechanism of decomposition

-The Mo_2 $(L^1)_5(OH)_2$ $(H_2O)_3$ complex proceeds in the following decomposition steps:

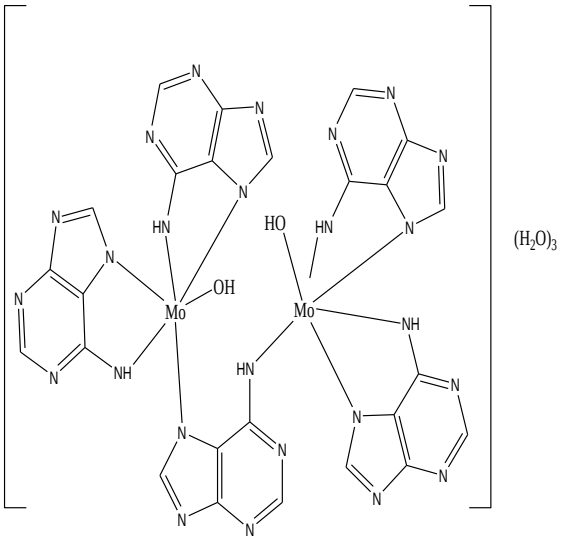

$-C_3H_4N_4O_3$

28.125 C-262.5 C

Exp(% 14.94)

Calc(%15.00)

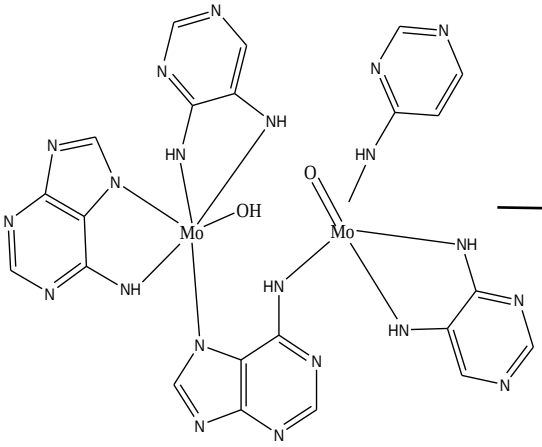

$-C_{19}N_4$

262.5 C- 470.625 C C

Exp(% 18.26)

Calc(%18.34)

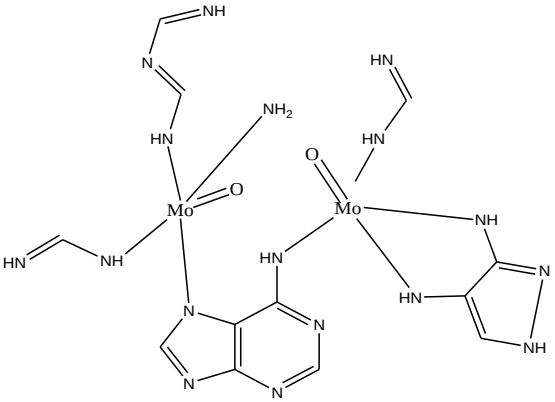

$-C_{13}H_{21}N_{14}$

470.625 C-800 C

Exp(% 39.26)

Calc(%38.87)

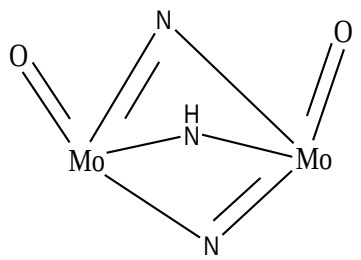

-However Cr_2 $(HL^1)_2(H_2L^1)$ (SO_4) $_2(H_2O)_7$, complex proceeds in the following decomposition steps:

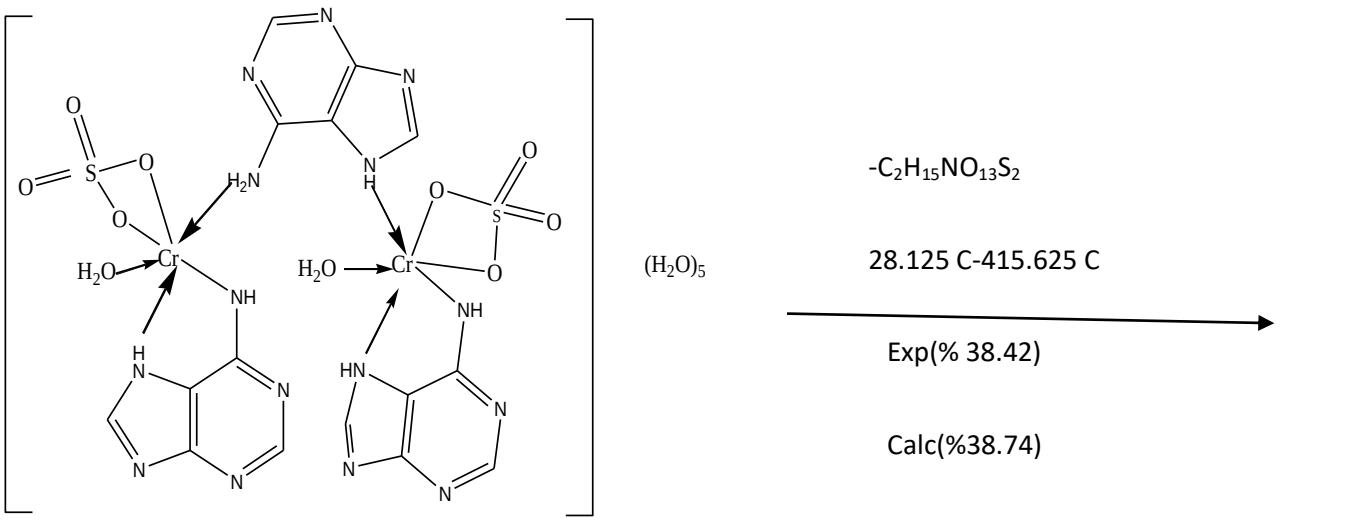

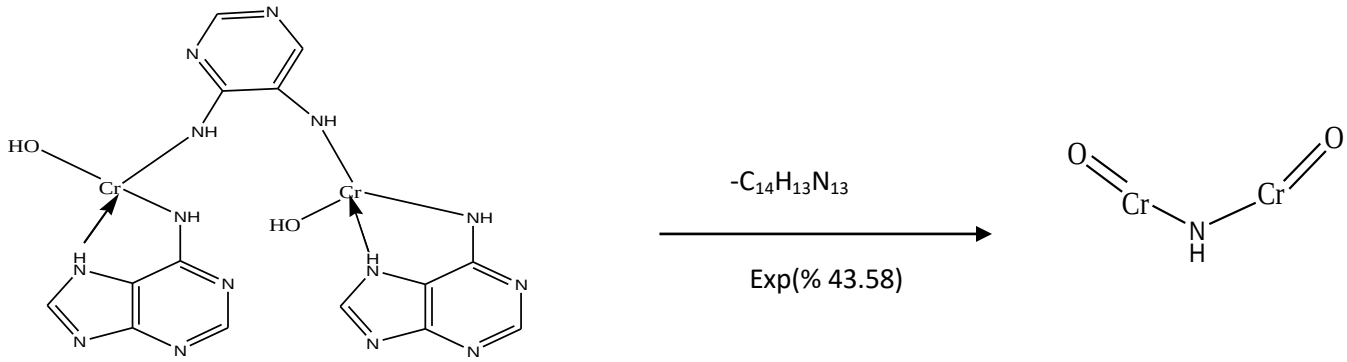

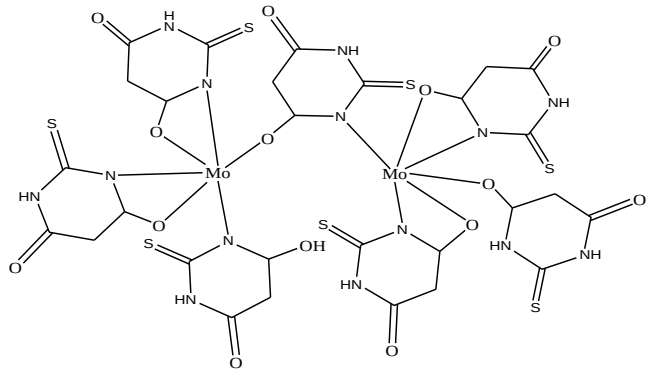

-6(CO)28.1 C-

234.38 C

Exp(%14.65)

Calc(%13.97)

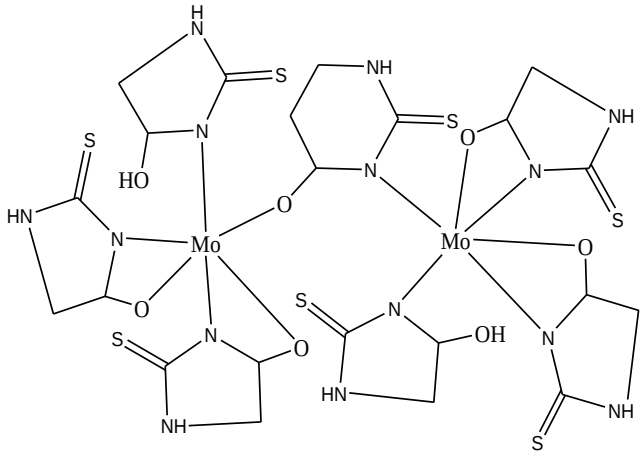

$-C_{18}H_{16}N_8O_4S_7$

234.38 C-800

Exp(%51.94)

Calc(%52.61)

2

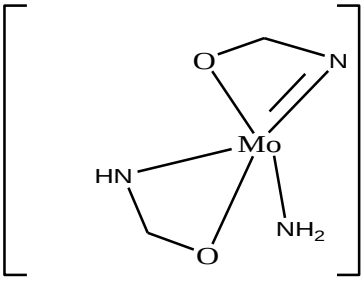

- Mn $(H_2L_2)_3Cl_2$ proceed in the following decomposition steps:

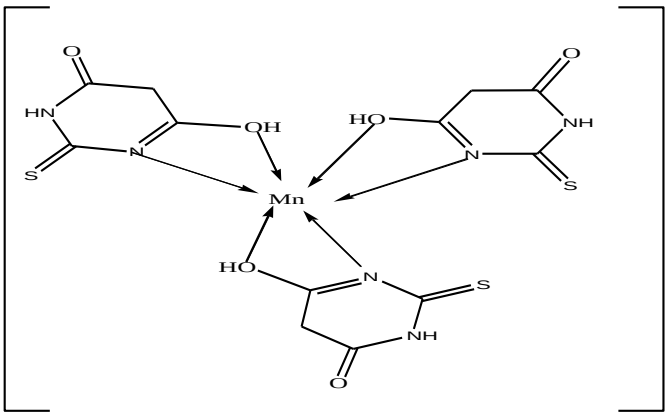

2Cl

$-C_2H_2O_3Cl_2$

46.9 C-275 C

Exp(%26.47)

Calc(%25.96)

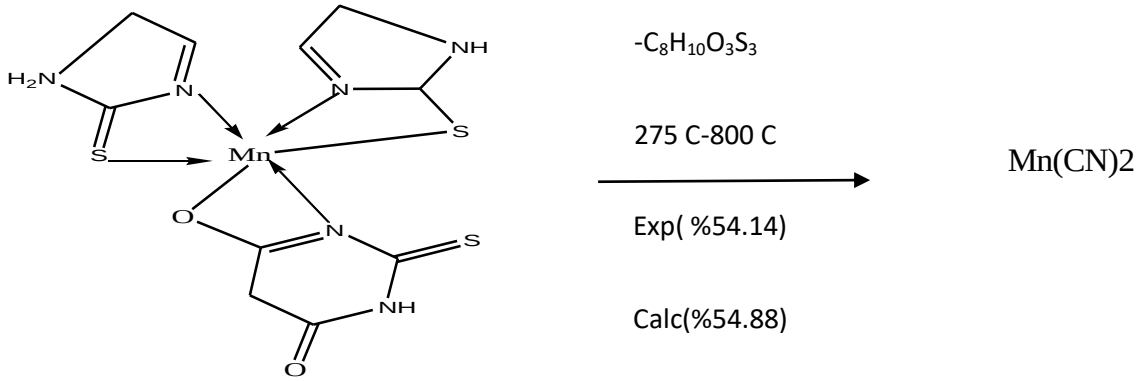

- Cr (H L_2)(L_2) $(H_2O)_3$ proceed in the following decomposition steps:

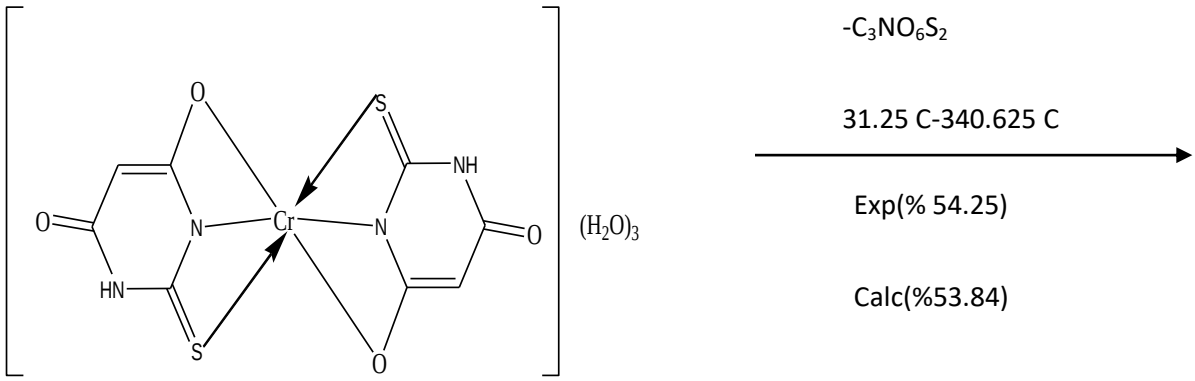

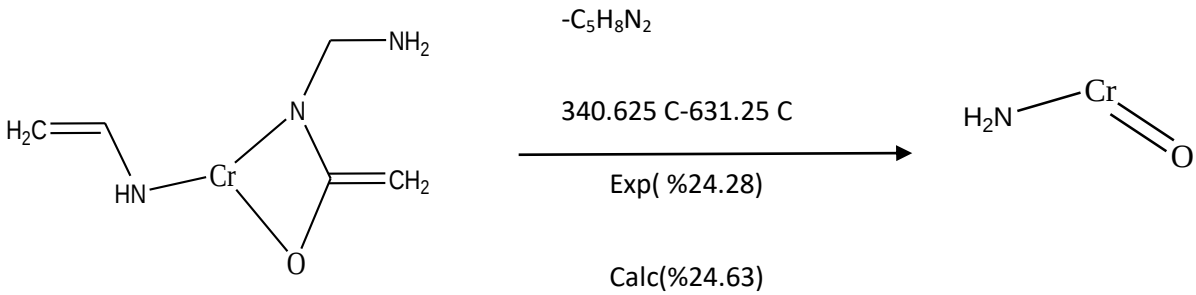

b) DTA studies

DTA thermal analysis were studied for the prepared complexes $Mo_2(L^2)_5(H\ L^2)_2$, Mn $(H_2L_2)_3Cl_2$, Cr (H L^2) (L^2) $(H_2O)_3$, Mo_2 $(L^1)_5(OH)_2$ $(H_2O)_3$ and Cr_2 (H $L^1)_2(H_2\ L^1)$ $(SO_4)_2(H_2O)_7$. Most of the DTA peaks (14 peaks) for five complexes are of endo behavior, and only four are of exo trend [$Mo_2(L_2)_5(HL_2)_2$(peak a), Mn $(H_2L_2)_3Cl_2$ (peak c), Mo_2 $(L^1)_5(OH)_2$ $(H_2O)_3$(peak a) and Cr_2 (H $L^1)_2(H_2\ L^1)$ $(SO_4)_2$ $(H_2O)_7$ (peak c).

The ln ΔT *versus* 10^3/T plots for the complexes: $Mo_2(L^2)_5(H\ L^2)_2$, Mn $(H_2\ L^2)_3Cl_2$, Cr $(H\ L^2)(\ L^2)\ (H_2O)_3$, $Mo_2\ (L^1)_5(OH)_2\ (H_2O)_3$ and $Cr_2\ (H\ L^1)_2(H_2\ L^1)\ (SO_4)\ _2(H_2O)_7$ respectively are given, where, Figures 3-7 gave best fit straight lines from which the activation energies (E_a) were calculated. The order of chemical reactions (n) was calculated *via* the peak symmetry method [35-37]. The reaction orders are 1, 1.5 and 2. The fractions appeared in the calculated order of the thermal reactions, (n), Table 6, confirmed that the reactions proceeded in complicated mechanisms.

The maximum and the minimum T_m values are 929 and 317° K, respectively. The value of the decomposed substance fraction, α_m, at the moment of maximum development of reaction (with $T=T_m$) being determined from the relation [38].

$$(1-\alpha_m) = n^{\frac{1}{1-n}}$$

It is of nearly the same magnitude and lies within the range 0.501-0.610.

The calculated values of the collisions number, Z, showed a direct relation to E_a. The maximum and minimum Z values are 0.628 and 0.088, respectively, let to suggest different mechanisms with variable speeds. The collisions number, Z, are calculated from the following equation [39,40]:

$Z=(\Delta\ E_a/RT_m)$ ß exp $(\Delta\ E_a/RT^2_m)$

Where R=molar gas constant.

ß=rate of heating

T_m=temperature of maximum or minimum peak

The entropies of activation $\Delta S^{\#}$, are calculated from the following equation [39]:

$Z=(K\ T_m/h\ )$ exp $\Delta S^{\#}$ R

K=Boltzman constant.

h=Planch's constant

The change of entropy values, $\Delta S^{\#}$, for all complexes, are nearly of the same magnitude and lie within the range -0.273 to -0.290 $kJK^{-1}mol^{-1}$, all are with –ve signs, Table 6. So, the transition states are more ordered, i.e., in a less random molecular configuration, than the reacting complexes.

The heat of transformation, $\Delta H^{\#}$, can be calculated [41]. All the $\Delta H^{\#}$ values are with –ve signs, Table 6. In general, the change in enthalpy ($\Delta H^{\#}$) for any phase transformation taking place at any peak temperature, T_m, can be given by the following equation:

$$\Delta S^{\#} = \Delta H^{\#} / T_m$$

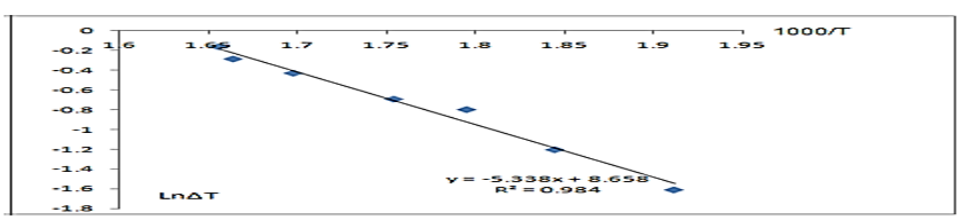

Figure 3. ln ΔT-10^3/T relationship for $Mo_2(L^2)_5(HL^2)_2$ complex

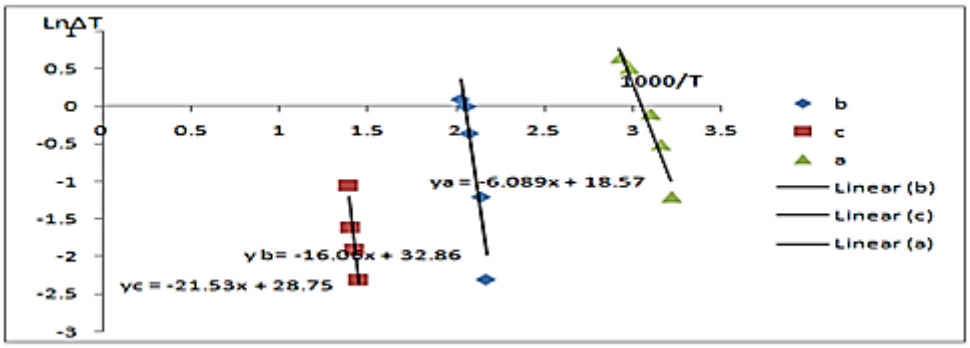

Figure 4. ln ΔT-10^3/T relationshipfor Mn $(H_2L^2)_3Cl_2$ complex

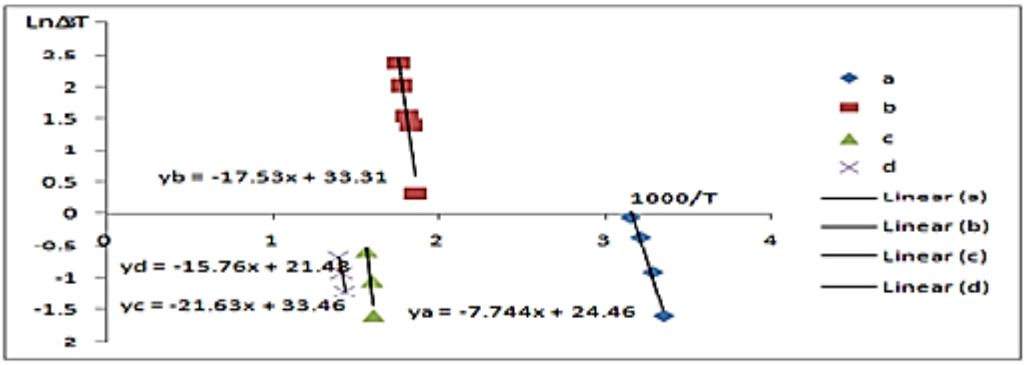

Figure 5. ln ΔT-10^3/T relationship for Cr $(H\ L^2)(\ L^2)\ (H_2O)_3$ complex

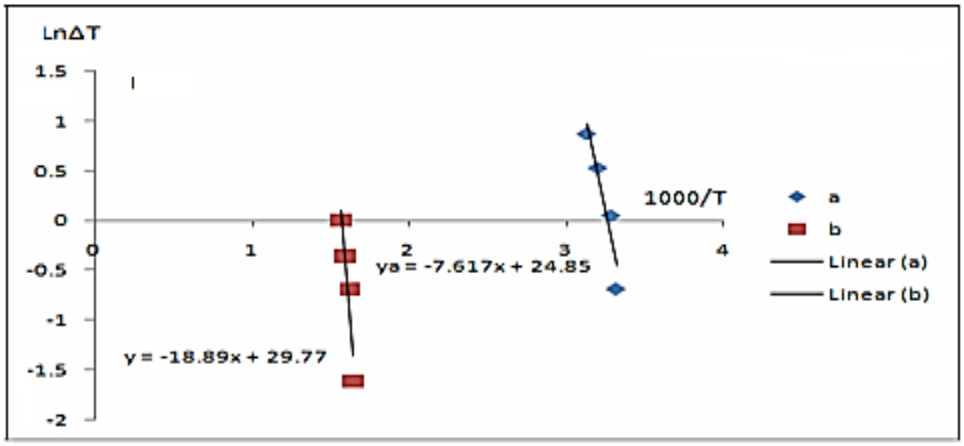

Figure 6. ln ΔT-10^3/T relationship for $Mo_2\ (L^1)_5(OH)_2\ (H_2O)_3$, complex

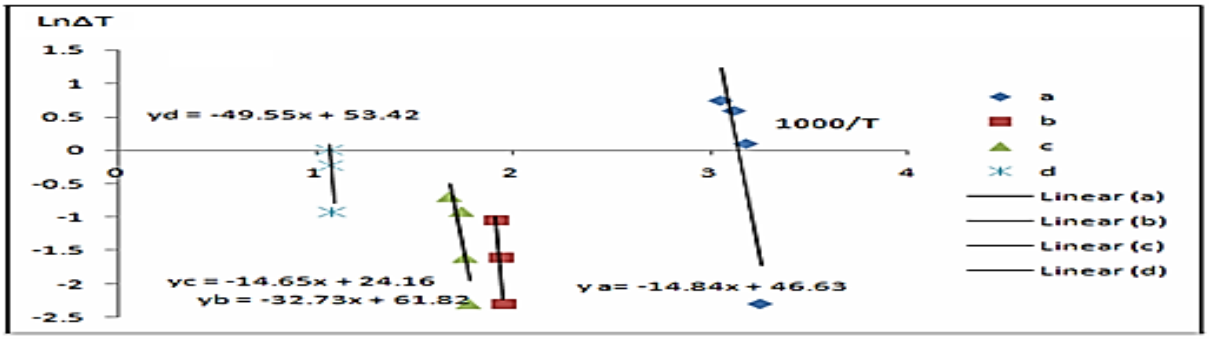

Figure 7. ln ΔT-10^3/T relationship for Cr_2 $(HL^1)_2(H_2L^1)$ (SO_4) $_2(H_2O)_7$ complex

Table 6. DTA thermodynamic parameters of the complexes

Complex	Peak (type)	Slope	ΔE_α	a	b	N	α_m	Tm (ºK)	Z	$\Delta S^\#$	$\Delta H^\#$
$Mo_2(L^2)z(HL^2)_2$	a(exo)	-5.338	44.38	1.5	1.5	1.26	0.589	604	0.088	-0.29	-175.221
Mn $(H_2L^2)_3Cl_2$	a(endo)	-6.089	50.624	0.3	0.6	0.891	0.653	342	0.178	-0.28	-95.606
	b(endo)	-16.06	133.523	0.3	0.3	1.26	0.589	494	0.325	-0.278	-137.135
	c(exo)	-21.53	179	0.4	0.5	10127	0.61	719	0.299	-0.281	-202.33
Cr $(H\ L^2)(L^2)(H_2O)_3$	a(endo)	-7.744	64.384	0.6	0.3	1.782	0.522	317	0.244	-0.276	-87.584
	b(endo)	-17.53	147.744	0.45	0.45	1.26	0.589	568	0.309	-0.279	-158.582
	c(endo)	-21.63	179.832	0.5	0.3	1.627	0.54	636	0.34	-0.279	-177.652
	d(endo)	-15.76	131.029	0.5	0.6	1.15	0.606	711	0.222	-0.284	-201.791
$Mo_2(L^1)_5(OH)_2(H_2O)_3$	a(exo)	-18.84	63.328	0.4	0.45	1.188	0.6	319	0.239	-0.277	-88.214
	b(endo)	-32.75	157.052	0.25	0.275	1.202	0.598	637	0.297	-0.28	-178.665
$Cr_2(H\ L^1)_2(H_2\ L^1)(SO_4)$ $_2(H_2O)_7$	a(endo)	-18.84	156.636	0.6	0.4	1.543	0.55	327	0.576	-0.269	-88.099
	b(endo)	-32.75	272.284	0.4	0.2	1.782	0.522	521	0.628	-0.273	-142.005
	c(exo)	-14.65	121.8	0.5	0.35	1.506	0.555	594	0.247	-0.281	-167.17
	d(endo)	-49.55	411.959	1	0.4	1.992	0.501	929	0.533	-0.279	-258.946

c) DSC studies

The Debye model [42-45]; is applied to describe capacity change over a large temperature range. The C_p can be represented as the following empirical form:

$C_p = aT + b$

By plotting C_p *versus* T, a straight line is obtained, thus, "a" and "b" parameters can be determined from the slope and intercept of the line, respectively, represented example Figure 8 and Table 7.

Further applications based on Debye model on the complexes are given from the scope of the following equations:

$C_p \cong C_v = \alpha T^3 + \gamma T$, $$\frac{C_p}{T} = \alpha T^2 + \gamma$$

Where, γ and α are the coefficients of electronic and lattice heat capacities, respectively. C_v is the heat capacity at constant volume which is assumed to be equal to C_p. Plots of Cp/T versus T^2 should yield straight lines with slopes α and intercepts γ, represented example Figure 8 and Table 8.

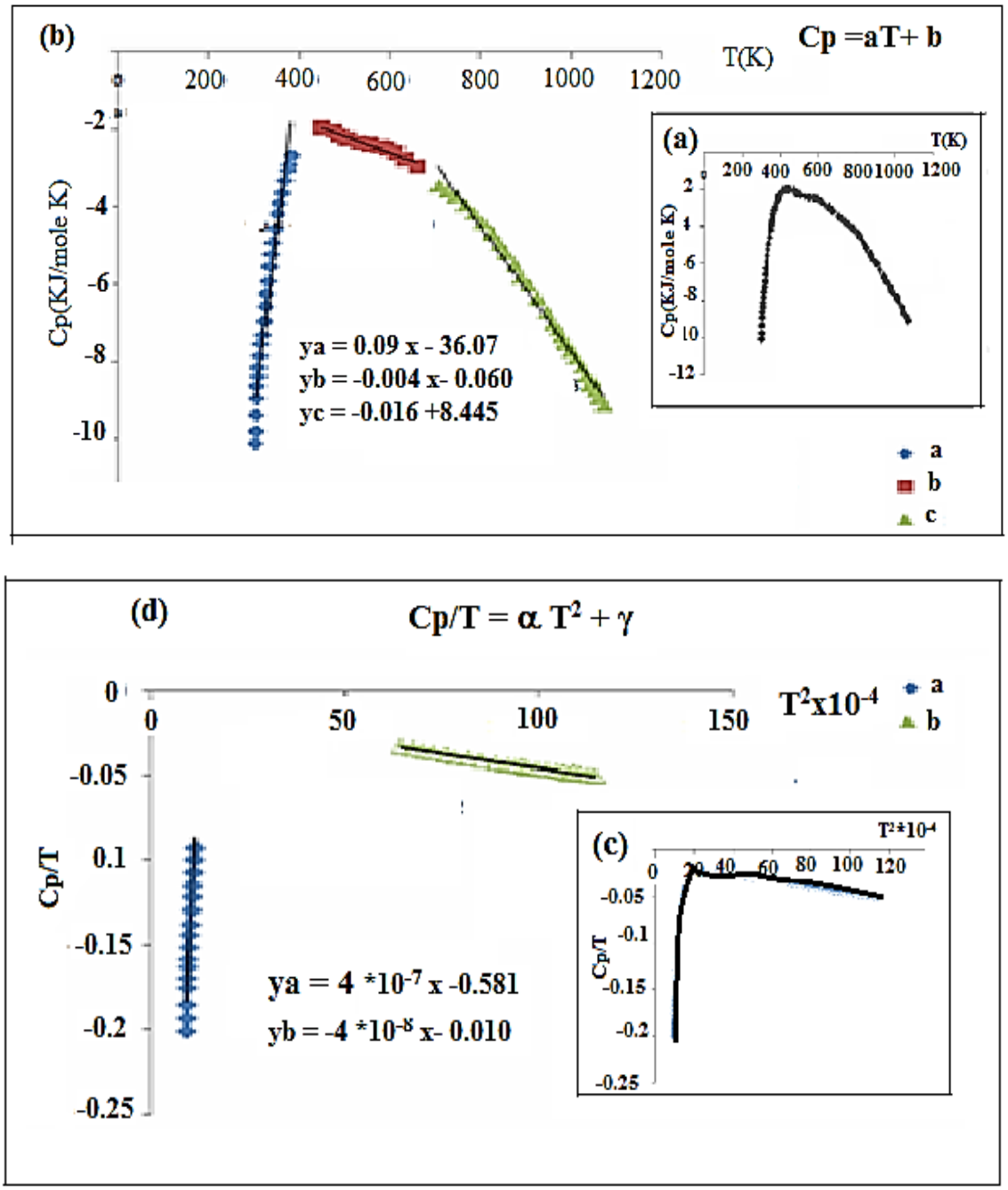

Figure 8. DSC curves of $Mo_2(L^2)_5(H\,L^2)_2$ complex dependence of specific heat and temperature.

Table 7. The slopes "a" and intercept "b" for DSC curves of selected complexes

Complex	a_1 [b_1]	a_2 [b_2]	a_3 [b_3]	a_4 [b_4]	a_5 [b_5]	a_6 [b_6]
$Mo_2(L^2)_5(H\,L^2)_2$	0.09 -36.07 302-381°K	-0.004 -0.06 449-633°K	-0.016 -8.445 706-1061°K			
$Mn\,(H_2\,L^2)_3Cl_2$	0.394 -166.1 303-376°K	-0.062 18.77 459-476°K	-0.023 0.006 544-565°K	-0.141 87.35 772-1064°K		
$Cr\,(H\,L^2)(\,L^2)\,(H_2O)_3$	0.335 -135.3 299-360°K	-0.019 0.085 414-495°K	-0.267 128.5 524-760°K	0.792 -472 568-577°K	-0.029 5.778 615-692°K	-0.095 56.32 771-1045°K
$Mo_2\,(L^1)_5(OH)_2\,(H_2O)_3$	0.458 -183.9 304-365°K	-0.032 4.672 45542°K	0.032 -14.91 583-622°K	-0.1 55.3 651-701°K	-0.063 27.37 680-1073°K	
$Cr_2\,(H\,L^1)_2(H_2\,L^1)\,(SO_4)_2(H_2O)_7$	0.338 -144.7 299-404°K	-0.25 1.38 469-554°K	-0.095 50.51 641-1073°K			

- $C_p = a\,T + b$

Table 8. The slopes "α" and intercept "γ" for DSC curves of selected complexes

Complex	**α_1 [γ_1]**	**α_2 [γ_2]**	**α_3 [γ_3]**	**α_4 [γ_4]**
$Mo_2(L^2)_5(H\,L^2)_2$	4^*10^{-6} [-0.58] $(302\text{-}361)^2$°K	2^*10^{-8} [-0.032] $(332\text{-}579)^2$°K	4^*10^{-8} [-0.010] $(804\text{-}1070)^2$°K	
$Mn\,(H_2\,L^2)_3Cl_2$	0.021 [0.001] $(303\text{-}382)^2$°K	0.001 [-0.045] $(418\text{-}459)^2$°K	-33.9 [-0.015] $(610\text{-}706)^2$°K	-60.64 0.001] $(805\text{-}1064)^2$°K
$Cr\,(H\,L^2)(\,L^2)\,(H_2O)_3$	0.018 [-0.045] $(299\text{-}373)^2$°K	0.003 [0.062] $(511\text{-}559)^2$°K	0.011 [-0.379] $(565\text{-}580)^2$°K	-43 [-0.002] $(791\text{-}1055)^2$°K
$Mo_2\,(L^1)_5(OH)_2\,(H_2O)_3$	0.02 [-0.329] $(304\text{-}388)^2$°K	0.002 [-0.034] $(583\text{-}622)^2$°K	-44.2 [-0.006] $(701\text{-}1073)^2$°K	
$Cr_2\,(H\,L^1)_2(H_2\,L^1)\,(SO_4)_2(H_2O)_7$	0.02 [-0.322] $(299\text{-}381)^2$°K	$6*10^{-5}$ [-0.024] $(554\text{-}613)^2$°K	-47.6 [-0.004] $(721\text{-}1073)^2$°K	

$$\frac{C_P}{T} = \alpha T^2 + \gamma$$

The Reaction of ^{18}F with Some of the Prepared Complexes

The reaction of ^{18}F with Mn $(H_2L^2)_3Cl_2$, Cr $(H\ L^2)(L^2)\ (H_2O)_3$, $Mo_2\ (L^1)_5(OH)_2\ (H_2O)_3$ and $Cr_2\ (HL^1)_2(H_2L^1)\ (SO_4)_2(H_2O)_7$ were studied in neutral, acidic and basic media, Table 9, represented example Figure 9. The reaction mixtures have been analyzed by TLC and a radiodetector to show the peaks at the plates. The determination of the extent of radiolabeling was done by thin layer chromatography using (95:5 water to acetonitril) solution as a solvent.

1) The TLC data of the ^{18}F with Mn $(H_2\ L^2)_3Cl_2$ complex at neutral, acidic and basic media are summarized in Table 9.

On monitoring the reaction of ^{18}F and Mn $(H_2\ L^2)_3Cl_2$ complex in neutral and basic medias two bands were appeared one of (R_f ~ 0.0) for unreacted ^{18}F [44] with % composition of (96.35 and 94.01) and the second of (R_f ~ 0.6) with % composition of (3.65 and 5.63) respectively, while one band was appeared in acidic medium of (R_f ~ 0) for free ^{18}F (i.e., no interaction happened between ^{18}F and Mn $(H_2L_2)_3Cl_2$ complex in acidic medium).

2) The TLC data of the ^{18}F with $Mo_2\ (L_1)_5(OH)_2\ (H_2O)_3$ complex at neutral, acidic and basic media are summarized in Figure 8 and Table 9.

Three bands were appeared of R_f (~0.0, ~ 0.4 and ~ 1.0) with % composition (94.08, 3.82 and 0.0) in neutral medium, (55.25, 30.56 and 10.9) in acidic medium and (89.07, 4.20 and 3.99) in basic medium respectively indicating that an interaction happened between the ^{18}F ion and $Mo_2\ (L^3)_5(OH)_2\ (H_2O)_3$ complex and new complexes were formed with R_f (~0.4 and ~1.0). The formation of the new complexes increased in acidic medium decreased in basic and neutral media.

A nuclciophilic substitution may be occurred and ^{18}F replaced one or more of the hydroxyl groups in $Mo_2\ (L^1)_5(OH)_2\ (H_2O)_3$ complex according to the following equations:

$$Mo_2\ (L^1)_5(OH)_2\ (H_2O)_3 + {}^{18}F^- \longrightarrow Mo_2\ (L^1)_5(OH)({}^{18}F)\ (H_2O)_3 + OH^-$$

$$Mo_2\ (L^1)_5(OH)_2\ (H_2O)_3 + 2\ {}^{18}F^- \longrightarrow Mo_2\ (L^1)_5\ ({}^{18}F)_2\ (H_2O)_3 + 2\ OH^-$$

The TLC data of the ^{18}F with $Cr_2\ (H\ L^1)_2(H_2\ L^1)\ (SO_4)_2(H_2O)_7$ complex at neutral, acidic and basic media are summarized in, Table 9.

On monitoring the reaction of ^{18}F and $Cr_2\ (H\ L^1)_2(H_2\ L^1)\ (SO_4)_2(H_2O)_7$ complex in neutral, acidic and basic media two bands were appeared one of (R_f ~ 0.0) for unreacted ^{18}F with % composition of (92.65, 95.50 and 91.82) and the second of (R_f ~ 0.4) with % composition of (0.17, 1.8 and 5.75) respectively. A third band of R_f ~ 0.75 appeared in acidic medium. The low percentage of the formed bands indicate the week interaction between ^{18}F and $Cr_2\ (H\ L^1)_2(H_2\ L^1)\ (SO_4)_2(H_2O)$ complex.

Table 9. Thin layer chromatography in (95:5, MeCN: H_2O) solution of ^{18}F with Mn $(H_2 L^2)_3Cl_2$, Mo_2 $(L^1)_5(OH)_2$ $(H_2O)_3$, Cr $(H L^2)_2$ $(H_2O)_3$ and Cr_2 $(H L^1)_2(H_2 L^1)$ $(SO_4)_2(H_2O)_7$ complexes in acidic, basic and neutral media

Complex	R_f	Specification	Neutral	Acidic	Basic
Mn $(H_2 L^2)_3Cl_2$	0.0-0.1 0.5-0.7	18F Coplexes (1)	96.35 3.65	94.99 -	94.01 5.60
Mo_2 $(L^1)_5(OH)_2$ $(H_2O)_3$	0.0-0.1 0.2-0.6 0.9-1.0	18F Coplexes (1) Coplexes (2)	94.08 3,82 -	55.25 30.56 10.9	89.07 4.2 3.99
$Cr_2(H L^1)_2(H_2 L^1)$ $(SO_4)_2(H_2O)_7$	0.0-0.1 0.2-0.6 0.7-0.8	18F Coplexes (1) Coplexes (2)	91.65 0.17 4.09	95.5 1.8 -	91.82 5.76 -
Cr $(H L^2)(L^2)$ $(H_2O)_3$	0.0-0.1	18F	92.65	95.5	91.82

CONCLUSION

From the previous studies we conclude:

1- The reactions proceeded in complicated mechanisms.

2- The transition states are more ordered than the reacting complexes

3- In the reaction of $^{18}F^-$ and $(H_2 L^2)_3Cl_2$, Mo_2 $(L^1)_5(OH)_2$ $(H_2O)_3$, Cr $(H L^2)(L^1)$ $(H_2O)_3$ and Cr_2 $(H L^1)_2(H_2 L^1)$ $(SO_4)_2(H_2O)_7$ complexes nuclciophilic substitution happened and $^{18}F^-$ replace $OH^- > Cl^- > SO_4^{-2}$ according to the electro negativity order.

Figure 9. TLC radio detector diagram for samples of the reaction of ^{18}F

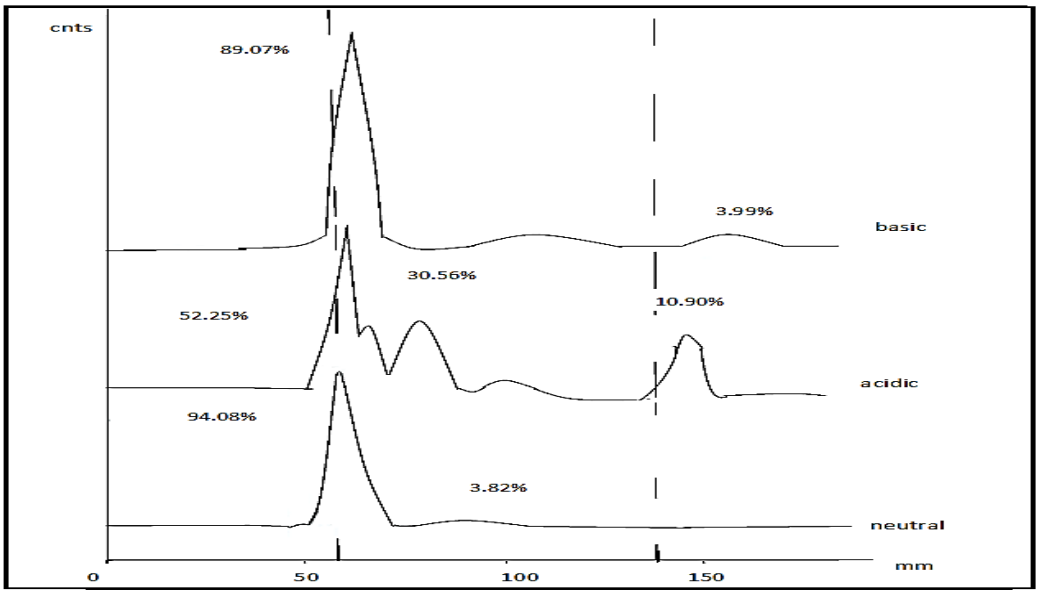

References

1. R Ramaekers; A Dkhissi; L Adamowicz; G Maes. *J Phys Chem*. **2002**, 106, 4502-4512.
2. W Saenger. *Principles of nucleic acids structure*. Springer, New York, **1984**.
3. MS Masoud; EA Khalil; AM Hindawy; AM Ramadan; *Canadian J Anal Sci Spectroscopy*. **2005**, 50(6), 297-310.
4. MS Masoud; SS Hagagg; EA Khalil. *Nucleotides and Nucleic Acids*. **2006**, 25(1), 73-87.
5. MS Masoud; EA Khalil; AM Ramadan. *J Anal Applied Pyrolysis*. **2007**, 78(1), 14-23.
6. RS Pilato; EI Stiefel; *Bioinorganic Catalysis*. ed. J Reedijk; Marcel Dekker; New York, **1993**, 131.
7. RH Holm. *Chem Rev*. **1987**, 87, 1401-1449.
8. R Hille. *Chem Rev* **1996**, 96, 2757-2816.
9. S Kumar; DN Dhar; PN Saxena. *J Sci Ind Res*. **2009**, 68, 181-187.
10. L Jr. Que; AE True. *Prog Inorg Chem*. **1990**, 38, 97-131.
11. JB Vincent; G Christou; *Adv Inorg Chem*. **1989**, 33, 197-257.
12. LR Codd; CT Dillon; PA Lay. *Prog Inorg Chem*. **2002**, 51, 145.
13. W Nt Mertz. *Nutr Rev*. **1975**, 33, 129.
14. F Holleman; AF Wiberg E; Wiberg N. *"Chromium"*. *Lehrbuch der Anorganischen Chemie* (in German) (91-100 ed.). Walter de Gruyter. **1985**, 1081-1095.
15. H Mickael; T Matthew; M Satoshi; W Zehong; Z Xiaomin; A broadly; L Thomas; CG Véronique; P Jan; *J Nature Chemistry*. **2013**, 5, 941-944.
16. B Priya; G Nitasha; RM Bhagwant; S Jaya; V Rakhee; W Ankit. *Ind J Nucl Med*. **2013**, 28(4), 200-206.
17. Yu S Varshavskii; EN In'kova; AA Grinberg; *Zh Neorg Khim* **1963**, 8(12), 3176.
18. K Molodkin; N Ya Esina; OI Andreeva. *Russian Journal of Inorganic Chemistry*. **2008**, 53(11), 1741-1744.
19. R Ilavarasi; MNS Rao; MRJ Udupa; *Indian Acad Sci*. **1997**, 109(2), 79-87.
20. JT Kloprogge; D Wharton; L Hickey; RL Frost. *J American Mineralogist*. **2002**, 87, 623-629.
21. M Zaki; GGJ Mohamed. *Spectrochimica Acta Part A*. **2000**, *56*, 1245-1250.
22. SL Stefan; BA El-Shetary; WG Hanna; SB El-Maraphy. *Microchem J*. **1987**, *35*, 51-65.
23. J Morvay; G Kozepesy; VJ Nikolasev. *Acta Pharm Hung* **1969**, *39*, 54.
24. V Nakamato; PJ Mc Carthy. John Wiley, New York, **1968,** 26.
25. KC Satpathy; AK Panda; R Mishra; AP Chapdar; SK Pradhan. *J Indian Chem Soc* **1994**, 71, 593.
26. JP Thielemann; A Ressler; T Walter; G Tzolova-Müller; C Hes. *J Applied Catalysis A: General*. **2011**, 399, 28-34.
27. M Fournier; C Louis; MM Che; M Chaquin; D Masure. *J Catal*. **1989**, 119, 400-414.
28. S Pal; P Ghosh; A Chakravorty. *J lnorg Chem*. **1985,** 24, 3704.
29. SK Chandra; P Basu; D Ray; SA Pal; Chakravorty. *J Inorg Chem*. **1990**, 29, 2423.
30. U Auerbach; T Weyhermuller; K Wieghardt; B Nuber; E Bill; C Butzlaff, AX Trautwein. *Inorg Chern* **1993**, 32, 508.

31. H Temel; U Cakir; B Otludil; HI Ugras; *J Synth React Inorg Met or Chem.* **2001**, 31, 8, 1323-1337.
32. RT Dutta; AE Syamal; *Elements of Magnetochemistry*, 2nd edn, **1993,** 98.
33. DN Sathyanarayana. Universities Press. **2001**.
34. JC Byun; CH Yoon; DH Mun; KJ Kim; YC Park; J Bull. *Korean Chem Soc*. **2006**, 27, 5.
35. HR Oswald; E Dubler. In: Wiedemann HG, eds. *Thermal analysis*, vol. 2. Basel: Birkhauser; **1972**.
36. ME Brown; M Maciejewski; S Vyazovkin. *Thermochim Acta*. **2000**, 355(2), 125-143.
37. MS Masoud; S Abou El-Enein; A Ramadan; A Goher. *J Anal App pyrolysis*. **2008**. 81(1), 45-51.
38. MS Masoud; DA Ghareeb; SS Ahmed. *Synthesis J Molc Str* **2017**, 1137, 634-648.
39. HE Kissinger; *J Anal Chem.* **1957**, 29, 1702.
40. HROswald; E Dubler. In: Wiedemann HG (Ed). **1972**, *Basel Switzerland*: Birkhauser.
41. ML Dhar; O Singh. *J Thermal Analysis and Calorimetry*. **1991**, 37, 259-265.
42. K Traore; *Analyse J Therm Anal.* **1972**, 4, 135-145.
43. C Degueldre; P Tissot; H Lartigue; M Pouchon; *Thermochim Acta*. **2003**, 403, 267-273.
44. MS Masoud; S Hagagg; AE Ali; NM Nasr. *J Mol Struct*. 2012, 1014, 17-25.
45. Yu S, *J Biomed Imaging Interv*. **2006**, 2(4), e57.